ELSEVIER

Journal of Nuclear Materials 241–243 (1997) 1190–1196

journal of nuclear materials

Experimental and calculated basis of the lithium capillary system as divertor material

N.V. Antonov [a], V.G. Belan [b], V.A. Evtihin [c], L.G. Golubchikov [d], V.I. Khripunov [a], V.M. Korjavin [d], I.E. Lyublinski [c], V.S. Maynashev [b], V.B. Petrov [a], V.I. Pistunovich [a,*], V.A. Pozharov [a], V.I. Podkovirnov [b], V.V. Shapkin [a], A.V. Vertkov [c]

[a] *RRC "Kurchatov Institute", Nuclear Fusion Institute, Moscow, Russia*
[b] *TRINITI Troitsk, Moscow region, Russia*
[c] *State Enterprise "Red Star", Moscow, Russia*
[d] *RF Ministry of Atomic Energy, Moscow, Russia*

Abstract

First results as experimental and calculated basis of a new concept are described in the paper. Experimental models of liquid lithium capillary structure have been tested at long-pulse high heat loads. The power loads on the capillary target up to 50 MW/m^2 were provided by an electron beam with electron energy ≤ 9 keV in a longitudinal magnetic field of 0.25 T. Seven experiments were performed with the different capillary targets. The effects of disruption discharges in tokamaks have been simulated by means of magnetized plasma flows with pulse length of 0.2 ms, electron density of 10^{22} m^3 and energy density up to 4 MJ/m^2. The plasma flow was generated by a quasistationary plasma accelerator and interacted with a lithium capillary structure. 2D modelling of the ITER divertor with a lithium target is presented as the first step in the validation of a new divertor concept. A lithium radiative divertor scenario has been examined for the ITER using DDIC95 code. First calculations have shown that thermal loads on the divertor plates are reduced down to 1.3 MW/m^2. The main power is radiated in the divertor.

Keywords: Fusion technology; Energy deposition; Low Z wall material

1. Introduction

The divertor is the highest power loaded element of the tokamak fusion reactor. The main portion of thermonuclear energy in the ITER is supposed to be irradiated to the walls of the divertor and of the main chamber when argon or neon are puffed into the divertor. The specific power load of the divertor plates should not exceed 5 MW/m^2 in a steady state operation and 15 MW/m^2 in pulsed mode with 10 s duration of pulses. Nevertheless up to now there is no self-consistent solution of the divertor problem because the heavy gas puffed in the divertor as well as the atoms of the divertor plate structural materials sputtered by the high energy particles will penetrate to the main reactor chamber and they can substantially impair the plasma burning regime.

In the DEMO reactor the situation is more complicated because the thermal loads on the divertor plates become essentially higher.

Here experimental and calculated results are given in the validation of a new divertor concept [1], based on the capillary structure applied for the cooling of the divertor plates by evaporation of lithium.

As validation of the new concept, the tests and study have been done with a lithium capillary system under electron beam impact at the specific power ratings up to 50

* Corresponding author. Tel.: +7-095 196 7012; fax: +7-095 943 0073; e-mail: vip@wowa.net.kiae.su.

0022-3115/97/$17.00 Copyright © 1997 Elsevier Science B.V. All rights reserved.
PII S0022-3115(96)00698-8

MW/m^2, and disruption discharges in tokamak have been simulated by means of plasma flows with energy density up to 4 MJ/m^2.

2. Lithium capillary targets

Three types of target have been developed and manufactured for these experiments. The targets are schematically shown in Fig. 1. The type 'a' target (Fig. 1a) was used in the ELU-9 [2] device with the vertical electron beam.

The type 'b' of the target was designed for the experiments in the SPRUT [2] and QSPA [3] devices with horizontal electron beam and plasma flow. Its design and structural materials were similar to those of the type 'a' target. The only difference was the horizontal position of the large storage vessel and of the target. The type 'c', Fig. 1c, was of different design. The target assembly was made of a rectangular tube with the internal cross of 5×20 mm^2 having internal arterial channels to reduce the capillary system pressure drop. Niobium alloy was taken as a structural material for the type 'c' target, the irradiated surface and the capillary filler were made of molybdenum.

The full wetting of the capillary system was ensured by degassing operation in high vacuum at 1000°C before the loading of the vessel with lithium. The wetting of the capillary system after the loading operation was accomplished in the vacuum annealing process during one hour at a temperature up to 800°C.

Targets for plasma disruption simulation had the same design and structure materials as horizontal type target 'b'.

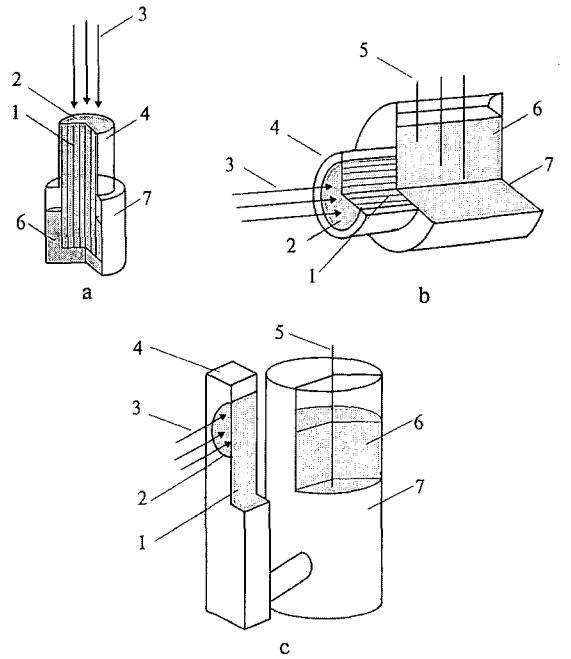

Fig. 1. Porous capillary system design options for (a) the vertical beam test, (b, c) the horizontal beam experiments: 1 – transport capillary system, 2 – capillary surface, 3 – electron beam, 4 – capillary target, 5 – level meter, 6 – liquid lithium, 7 – supply vessel.

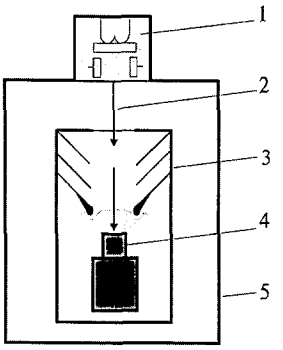

Fig. 2. The ELU-9 experiment scheme: 1 – electron beam source, 2 – electron beam, 3 – lithium vapor condenser, 4 – target, 5 – vacuum vessel.

3. Electron beam experiments

The experiments were performed in two devices in the vertical electron beam welding machine ELU-9 with a maximum power of 10 kW and in the SPRUT device with a 20 kW steady state horizontal electron beam in a longitudinal 0.25 T magnetic field [2]. The schemes of the experiments are given on Figs. 2 and 3. In both cases the electron beams were generated with tungsten cathodes and were accelerated to an energy up to 9 keV. The beams were transported to vacuum chambers equipped with refrigerating condensers. In the ELU-9 the condenser was not cooled. In the SPRUT device the condenser had forced water cooling and it was designed to condense lithium evaporated from the surface of the capillary system in order to limit the lithium ion flux into the electron gun.

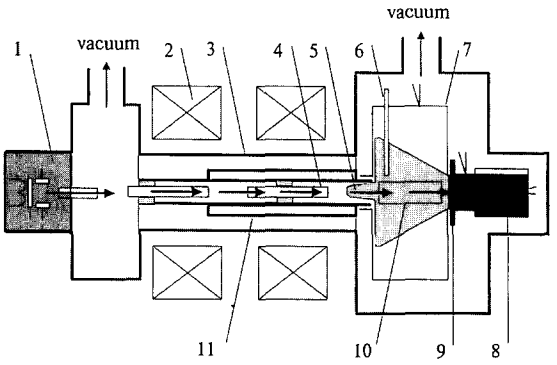

Fig. 3. The SPRUT experiment scheme 1 – electron beam source, 2 – magnetic system, 3 – vacuum vessel, 4 – differential vacuum resistance, 5 – electron beam, 6 – Langmuir's probe, 7 – lithium vapor condenser, 8 – target, 9 – capillary surface, 10 – viewing window, 11 – water cooling condenser.

In the SPRUT experiments, the electron beam leaving the condenser passed into the next zone surrounded with a non-cooled cylindrical shield. The lithium capillary target was mounted in it, the evaporating surface being turned to the electron beam. The evaporated lithium was condensed in the condenser and in the shield cylinder. The shield had a slot for optical observations and for video registration of the lithium radiation.

The experiments were made at a pressure of 10^{-3} Pa in the chamber. The current density radial distribution in the beam was measured with a moving probe in the SPRUT special experiments. The beam diameter values at the irradiated surface were 18 mm and 15 mm. In the ELU-9 the beam cross section was 5×9 mm. The following diagnostic methods were used in the SPRUT experiments with capillary targets: monitoring of the integral spectrum radiation of lithium atoms and ions in the vicinity of the receiving surface; video recording of the process of the beam-target interaction in time; measuring the gun accelerating voltage, the beam current and the target current values as functions of time; ion saturation current measurement with a Langmuir probe at 10 to 20 V bias in the plasma cloud at 7 cm from the evaporating surface; temperature measurements with thermocouples in the structural elements.

4. Experimental results

A molybdenum target 20 mm in diameter and 40 mm in thickness was used as a reference for comparison of the irradiation results on the capillary targets with other objects. This target was irradiated with an electron beam at 8 keV with a specific power of 20 MW/m^2 during 20 s. The result was the surface melting of the target, a crater of more than 1 mm in depth being formed.

The study of the type 'a' target was performed using the vertical electron beam (Fig. 2) and two other targets ('b' and 'c') were used in the horizontal beam experiments (Fig. 3). Two tests were made in the first case, and seven experiments were performed in the second one. Two targets in the first case were pre-heated up to 300°C and were exposed for 20 s and 30 s at the thermal load up to 30 MW/m^2 till full evaporation of the lithium. The first experiment carried out on the SPRUT device with the type 'b' target had a long duration, 10 min, at a low specific power of 5 MW/m^2. The lithium evaporation from the target surface during the experiment was followed by its free flowing out because of the non-compensated thermal loads and the capillary pressure. This has led to the drying of the target and its final damage. In the second experiment the specific power reached a maximum value of 50 MW/m^2 in the first five seconds. Then the load was lowered and was controlled at the 30 MW/m^2 level during the following 15 s, and at the 15 MW/m^2 level during 10 s and for the last 4 s it was raised up to 30 MW/m^2. The total time of continuous testing was 34 s, and the test was stopped because of the electron gun failure.

The capillary system was changed for the next three experiments. The type 'c' targets were manufactured on the basis of a rectangular niobium tube filled with a molybdenum capillary structure.

These experiments showed that in each case there was a normal operation phase and a damage of the target depending on the specific power rating of the beam. The analysis of the video recordings, integral radiation signals and the temperature of the receiving elements made it possible to identify the damage start moment. At the first phase of the target operation an intensive crimson light was observed. The molybdenum mesh damage start was identified as the white sparks appeared. In the third experiment the target was damaged in the last exposition period during 20 s. The system was dried completely because of the lithium evaporation and its flowing out. In the fourth and in the fifth tests the target was operating for 15 s and for 30 s at a specific power of 20 MW/m^2. The following sharp power rise up to 30 MW/m^2 caused quite rapid drying of the capillary system. We suppose that insufficient capillary pressure in this type of target was the cause of this phenomenon.

Thus the tests of the type 'c' capillary target have shown that a steady state heat removal was maintained at specific power rates from 15 to 20 MW/m^2 with the tube thickness 5 mm and the beam diameter 15 mm. The target is dried when the power rises over 20 MW/m^2 and the target is damaged. In the sixth experiment the power load did not exceed 25 MW/m^2, and the duration of irradiation was about 80 s. The irradiated surface in the target was not damaged Fig. 4. The seventh experiment carried out on the SPRUT device with the type 'b' target had a long duration, about 10 min at a low thermal load of ≤ 5 MW/m^2. Then

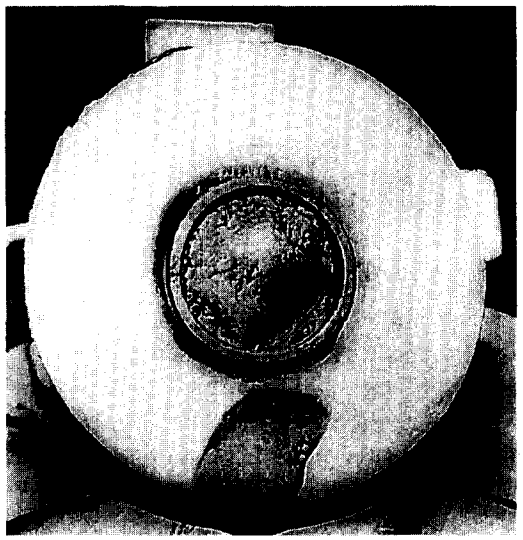

Fig. 4. Capillary target view after the sixth experiment.

the thermal load was increased up to 20 MW/m^2. The irradiated surface in the target was dried and damaged.

Thus different types of open lithium capillary structure were tested under intensive electron beam impact at the first time. Important data were obtained concerning the lithium capillary target operation under the thermal loads of the tokamak divertor. Further study of the optimum parameters of the lithium capillary structure is needed to find necessary design options.

5. Disruption simulation experiments

The effects of disruption discharges in tokamaks have been simulated by means of magnetized plasma flows, generated by quasistationary plasma accelerator QSPA, Fig. 5, interacting with lithium capillary structure. Experimental models of capillary structure, Fig. 1b, for liquid metal fusion reactor divertor simulation have been designed, manufactured and tested in order to estimate the behavior and possibilities of plasma facing components based on the lithium capillary system at disruptive high heat loads. In principle the capillary-pore system with liquid lithium has the capability of absorbing the energy under plasma disruptions without failure. The target was placed in the central part of the magnetic solenoid. The plasma flow parameters were: plasma density $n_e \approx 1$–2 10^{16} cm^{-3}, temperature $T_e + T_i \cong 30$ eV, magnetic field in plasma $B \cong 1$ T, energy density $Q \cong 4$ MJ/m^2, time duration of pulse $t \cong 200$ μs, diameter of plasma flow $\cong 80$ mm, plasma pressure $P \cong 4$ atm. The plasma density distribution near the target was measured by a Mach–Zehander argon laser ($\lambda = 5145$ Å) interferometer [3]. Use of a high speed camera provided a opportunity to obtain pictures with a time resolution $\cong 2/\mu$s. The spectroscope [3] with time and space resolution was used to measure the thickness of a layer evaporated material of the target. The split of the spectroscope was installed perpendicular to the target surface. Thus it was possible to evaluate the thickness of a radiating layer on the intensity of the spectral line

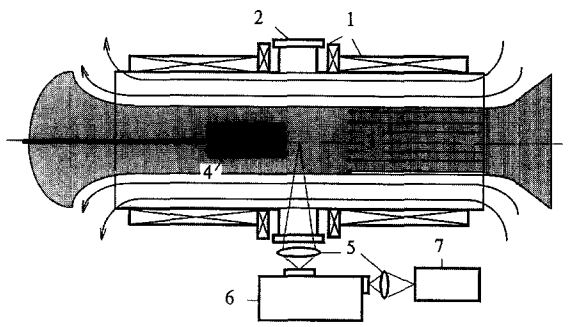

Fig. 5. The QSPA experiment scheme: 1 – magnetic coils, 2 – diagnostic window, 3 – plasma flow, 4 – target, 5 – lens, 6 – spectroscope, 7 – polychromator.

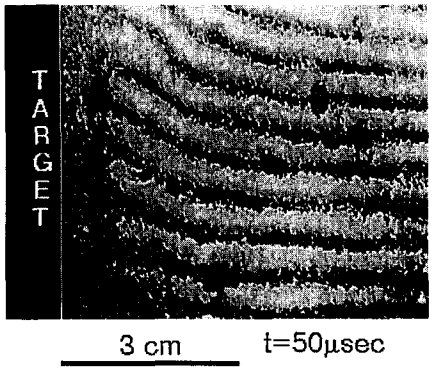

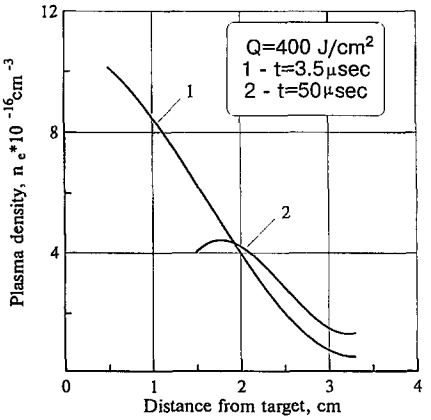

Fig. 6. Laser interferogram and plasma density distribution near the target.

[3]. The measurements were done on line LiI, $\lambda = 6103.6$ Å. The space resolution was ≈ 10 mm.

6. Experimental results and discussion

The high energy plasma flow interacted with the lithium capillary target, and a dense plasma layer is formed in

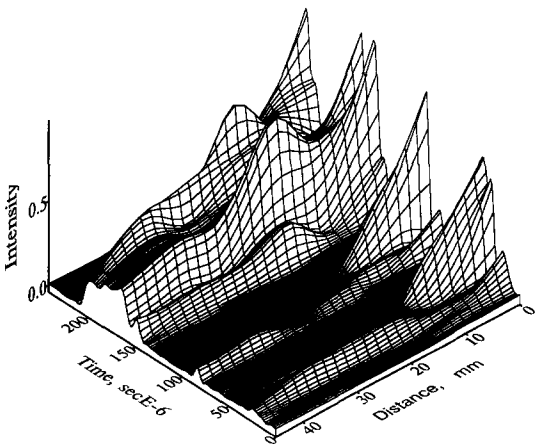

Fig. 7. Radiation intensity of neutral lithium as a function of distance from the target and time.

front of the target. From interferograms it is visible that at 5 μs the plasma density reaches $n_e = 10^{17}$ cm^{-3}. Then the density reduces and in front of the target surface a opaque layer $\delta \approx 1$–1.5 cm is formed. It may be explained by turbulence processes in the this layer. The plasma density distribution similar curve 2 (Fig. 6) is observed during all processes of interaction. To study the plasma layer formation and structure measurements of space distribution plasma density and intensity of radiation on the line LiI $\lambda = 6103.6$ Å in front of the target were done. The spectral researches of the plasma radiation from the target area show that there is strong radiation of neutral lithium on the line LiI. The measurement results of the neutral lithium layer thickness in front of the target are shown in Fig. 7. One can see that the evaporated neutral lithium emerges in about 10 μs after start-up of the plasma flow interaction with a target at a distance of about 1 cm from it. By the time $t \cong 200$ μs the layer becomes 4.5 cm thick. The pulsation of radiation can be explained by the plasma flow density change, since the intensity of radiation also depends on the electron density.

Thus the experiments show that a dense plasma layer, 1–1.5 cm thick, $n_e \cong 10^{17}$ cm^{-3}, is formed in front of a target. The main part of the plasma flow energy is absorbed and radiated in this layer which plays the role of a shielding layer. A small part of liquid lithium in the target is evaporated from it at each shot. The target remained undamaged even after six operating shots. A special target consisting of a molybdenum mesh without liquid lithium was destroyed by the plasma flow after a single shot.

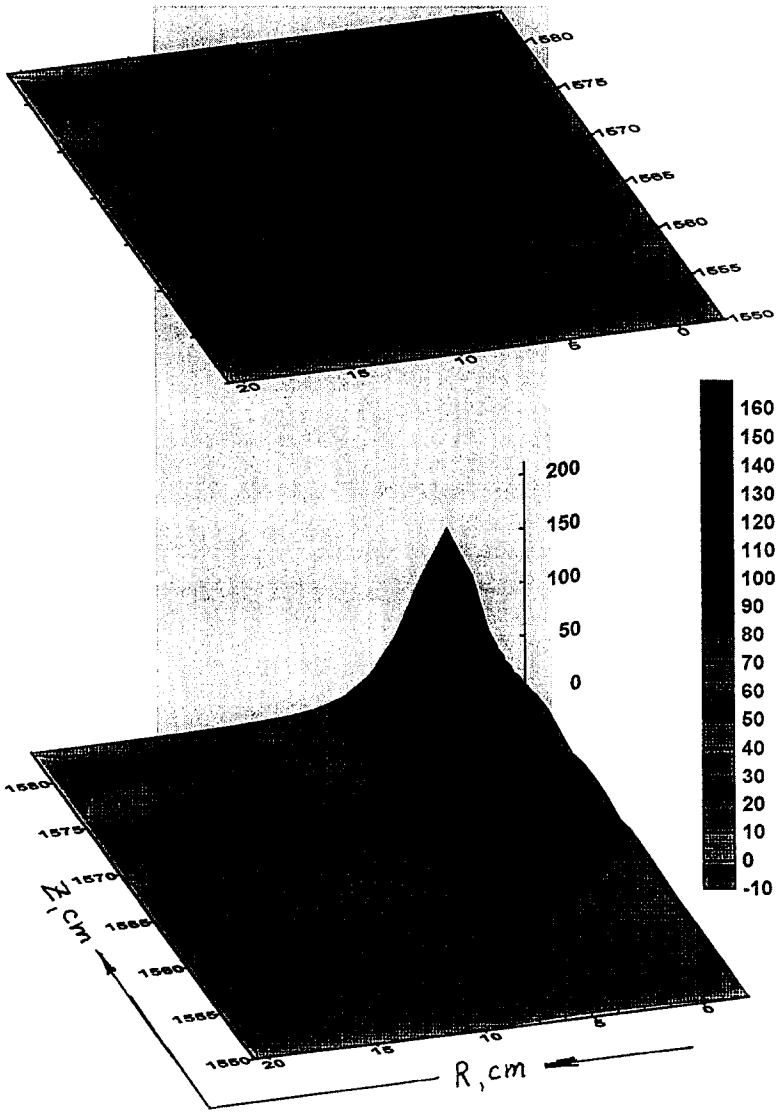

Fig. 8. The spatial distribution of the lithium radiation intensity (MW/m^2) calculated for the ITER parameters (see p. 16).

7. 2D ITER divertor modelling

2D-hydrodynamic code, DDIC95 [4], has been used to simulate a lithium target effect of plasma parameters in the ITER. This code has been specially produced to simulate the behavior of the main plasma and that of impurities, at their arbitrary densities in a real divertor geometry. The self-consistent simulation of a background plasma, neutral gas and impurities is a specific feature of this code. The impurities are considered in a multi-fluidal approximation, when each charged state is simulated by a separate fluid.

The lithium flow for the ITER parameters is determined by a heat plasma flow incident onto the plate. Lithium particles entering the material surface from the plasma are practically not reflected from it. In the simulation the material surfaces are assumed to be lithium particles adsorbing onto the surface.

Modelling has been done for typical ITER parameters: energy flow to the divertor layer 160 MW; electron density at the separatrix 6×10^{13} cm^{-3}; flux limit factor 0.21.

Results of the simulation are given as data near the x-point (D^+/T^+ ion density $n_i^x = 10.7 \times 10^{13}$ cm^{-3}; electron density $n_e^x = 18.2 \times 10^{13}$ cm^{-3}; ion and electron temperature $T_i^x = 37.7$ eV, $T_e^x = 105$ eV; $Z_{eff}^x = 1.83$) and on the divertor target: $n_i^d = 0.1 \times 10^{13}$ cm^{-3}, $n_e^d = 6.77 \times 10^{15}$ cm^{-3}, $T_i^d = 1.4$ eV, $T_e^d = 1.4$ eV, $Z_{eff}^d = 1.0$.

The main power which enters the divertor is radiated in the vicinity of the divertor plates by the lithium neutrals which screen the target, reducing the power flow density onto the lithium target to 1.3 MW/m^2. The spatial distribution of lithium radiation intensity is given in Fig. 8. Fig. 9 shows the lithium ions density distributions along the separatrix from the target to the symmetry plane, and the radial distribution in the symmetry plane. The lithium ions Li^+ and Li^{+2} density are concentrated in the vicinity to the divertor plate. A noticeable fraction of the Li^{+3} ions density only attains the x-point. In the symmetry plane the Li^{+3} ion maximal density is about 10^{10} cm^{-3}. The maximal $Z_{eff} \leq 1.9$ is attained in the divertor region, and it is considerably reduced in the space between the x-point and the symmetry plane.

The calculations show that the thermal loading onto the divertor plates is essentially reduced without addition of any heavy impurities at an electron density at the separatrix in the symmetry plane of $n_e^s = 6 \times 10^{13}$ cm^{-3}. The shielding of the target by lithium evaporation is realized.

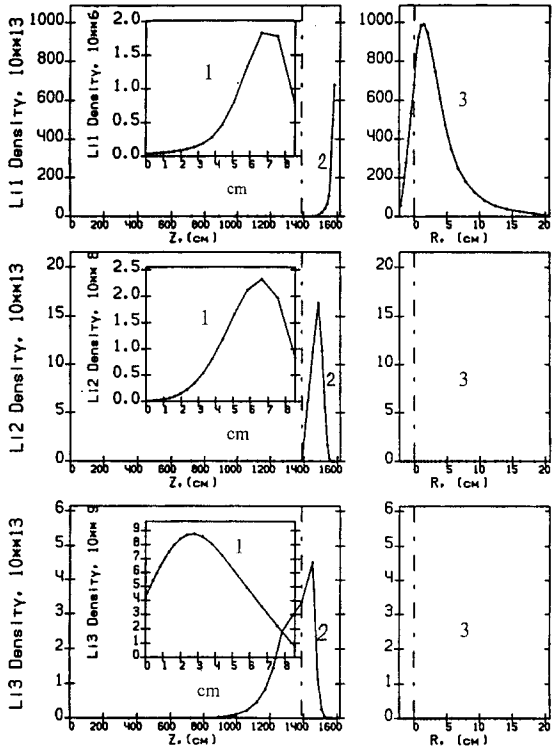

Fig. 9. The spatial distribution of the lithium ions density calculated for the ITER parameters (see p. 18): 1 – radial distribution in the symmetry plane of the ITER magnetic geometry; 2 – distribution along the separatrix; 3 – radial distribution on the divertor plate.

8. Conclusions

For the first time the experimental and calculated basis of an open lithium capillary-pore structure for a new divertor concept in a tokamak-reactor has been studied. This concept assumes the evaporational–radiational cooling highest loaded elements of the divertor.

The lithium capillary target has been successfully tested at a specific thermal load up to 50 MW/m^2 during 5 s. Long tests have been performed at 20 MW/m^2 and 30 MW/m^2 for 60 s and 30 s, and at 5 MW/m^2 for 10 min. These tests have shown the lithium capillary-pore structure to be promising because of its high heat removal capacity in a fusion reactor as well as in other devices.

Experiments simulating the disruption conditions in a tokamak, at an energy density up to 4 MJ/m^2 and at a pulse duration of 0.2 ms, have shown the opportunity of lithium capillary targets to withstand high pulsed loadings and to operate for a long time without destruction of a capillary-porous structure. The experiments show that in front of the target as a result of magnetized plasma flow a dense plasma layer, $n_e \geq 5 \times 10^{16}$ cm^{-3}, is formed. The main part of the plasma flow energy is absorbed and radiated in this layer, which plays a role as shielding layer.

2D modeling of the ITER divertor with the lithium target is done as the first step in the validation of a new divertor concept. The lithium radiative divertor scenario has been examined for ITER using DDIC95 code. The calculations have shown that thermal loads on the divertor plates are reduced down to 1.3 MW/m^2. The main power

entering the divertor is radiated on the baffles in the divertor.

References

[1] L.G. Golubchikov, V.A. Evtikhin et al., J. Nucl. Mater. 233–237 (1996) 667.

[2] V.I. Pistunovich, A.V. Vertkov et al., J. Nucl. Mater. 233-237 (1996) 650.

[3] V.G. Belan, V.F. Levashov et al., J. Nucl. Mater. 233–237 (1996) 763.

[4] V.A. Pozharov, report of the Fourth ITER Divertor Phisics and Database Expert Group Workshop, San Diego, CA, March 11–15, 1996.